Electronic Supplementary Material (ESI) for Nanoscale.

Supplemental Information for "Surface charge governed ionic blockade in angstrom-scale latent track channels"

Yanbo Xie,[1,2,*] Deli Shi,[2] Wenhui Wang,[2] and Ziheng Wang[2]

[1]*School of Aeronautics and Institute of Extreme Mechanics, Northwestern Polytechnical University, Xi'an, 710072, China*

[2]*School of Physical Science and Technology, Northwestern Polytechnical University, Xi'an, 710072, China*

[*] ybxie@nwpu.edu.cn

CONTENTS

I. FABRICATION OF THE LATENT TRACK ANGSTROM-SCALE PORES

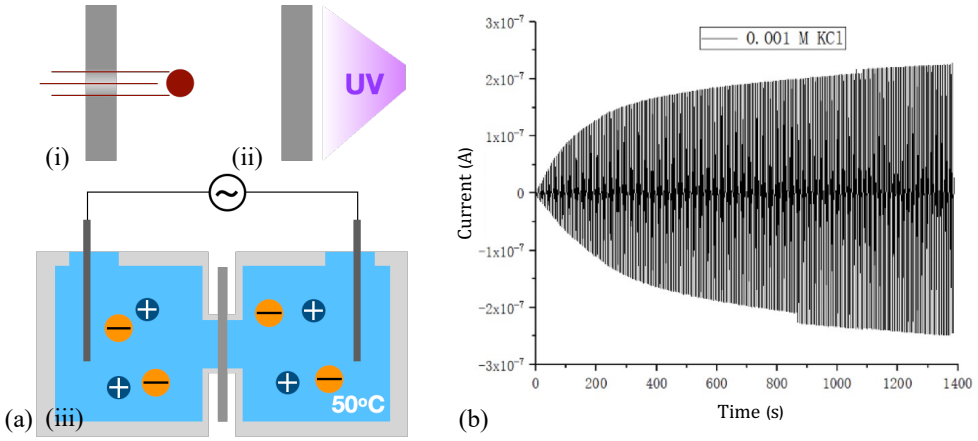

FIG. S1. (a). The schematic picture of channel fabrication. (b). The current measurement during voltage scanning.

Figure S1. (a) represents the procedure to fabricate the latent track nanochannels. First, the polymer films (PET) were irradiated by heavy ions (Kr) with energy over 1 MeV/u. The polymer chains were damaged along the ion track trajectory forming radiolysis products. The films were then placed under UV exposure for over 30 mins for both sides. Finally, the polymer films were clamped in two chambers, filled with KCl electrolyte solutions with concentration of 1mM. The chambers were placed in a water bath remaining the temperature of solutions at 50^oC, which help to remove of the radiolysis products. Two Ag/AgCl electrodes were placed in the chambers, connecting to a pico-ammeter (Keithley 6482), to monitor the conductance change of the polymer films. (b). gives an example of the I-V curves when starting to fabricate the latent track nanochannels. The conductance rapidly increases as time passes at beginning. However, gradually getting to a saturated value after 10 mins. To make sure the every latent channel were fabricated in the same condition, we keep the scanning in KCl solution for 25 mins, until the conductance turns to be saturated.

II. TYPICAL I-V CURVES

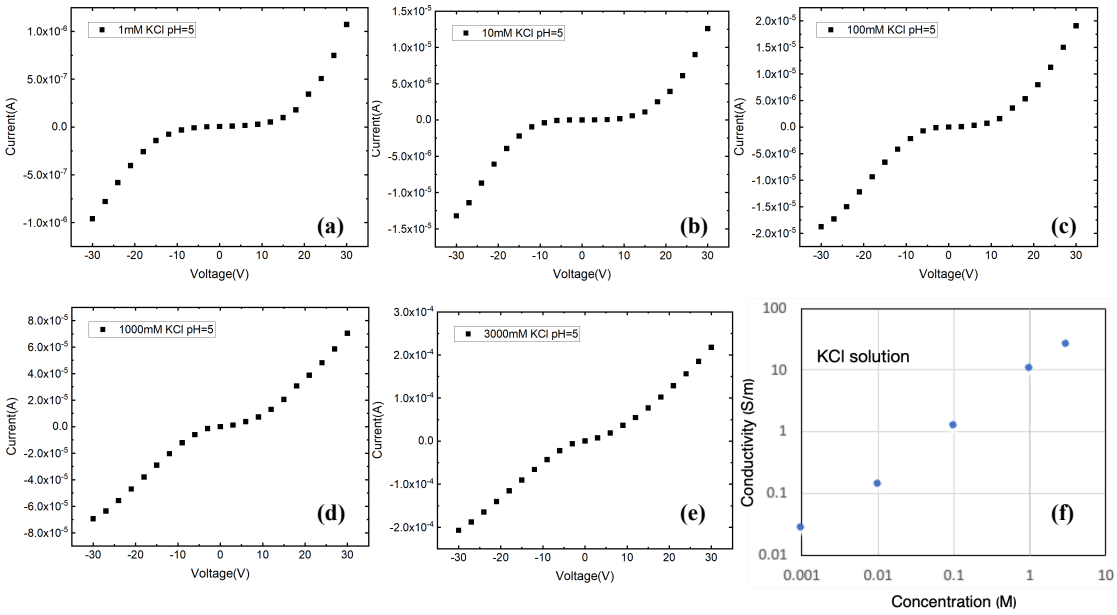

FIG. S2. (a). the typical I-V curves of KCl solution in various concentrations, from 1mM (a), 10mM (b), 100mM (c), 1M (d) and 3M (e). (f) indicates the conductivity change as a function of the concentration measured in the experiments.

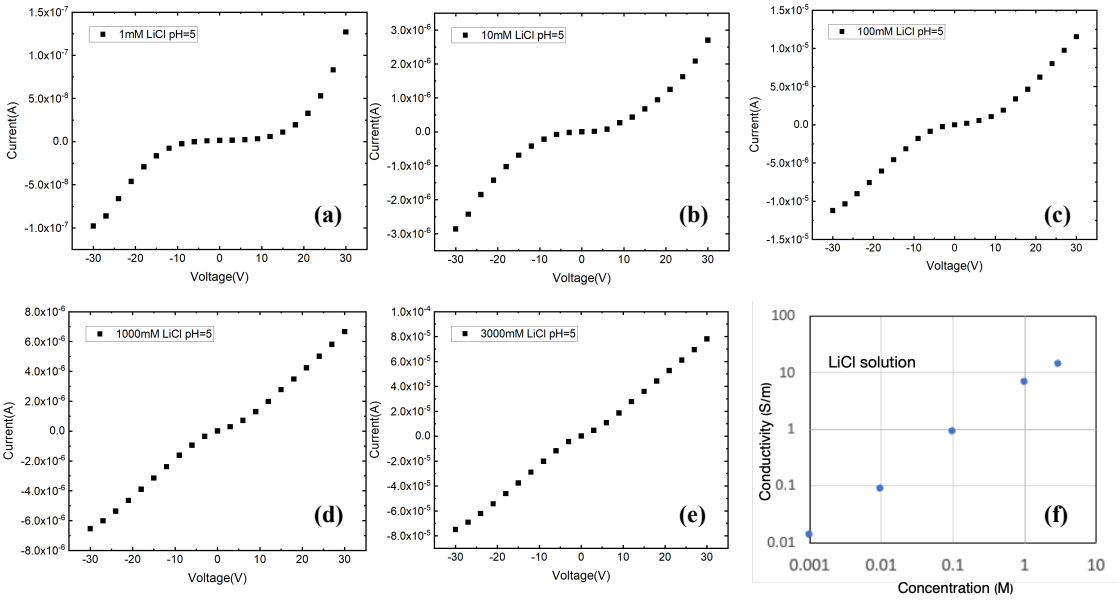

FIG. S3. the typical I-V curves of LiCl solution in various concentrations, from 1mM (a), 10mM (b), 100mM (c), 1M (d) and 3M (e). (f) indicates the conductivity change as a function of the concentration measured in the experiments.

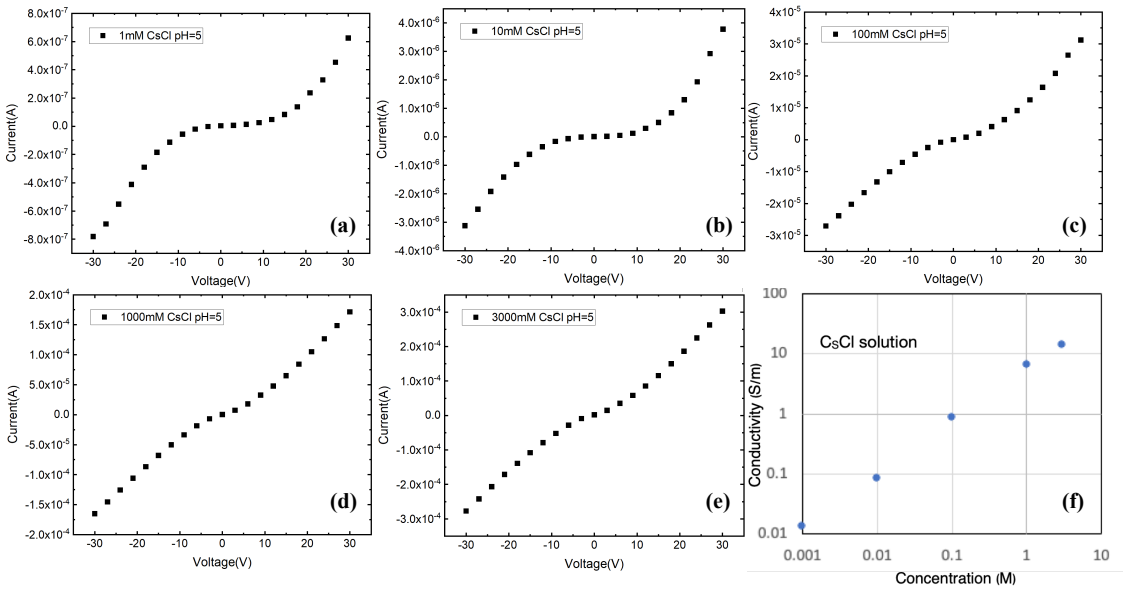

FIG. S4. the typical I-V curves of CsCl solution in various concentrations, from 1mM (a), 10mM (b), 100mM (c), 1M (d) and 3M (e). (f) indicates the conductivity change as a function of the concentration measured in the experiments.

III. THE CRITICAL VOLTAGE OF CONDUCTANCE TRANSITION

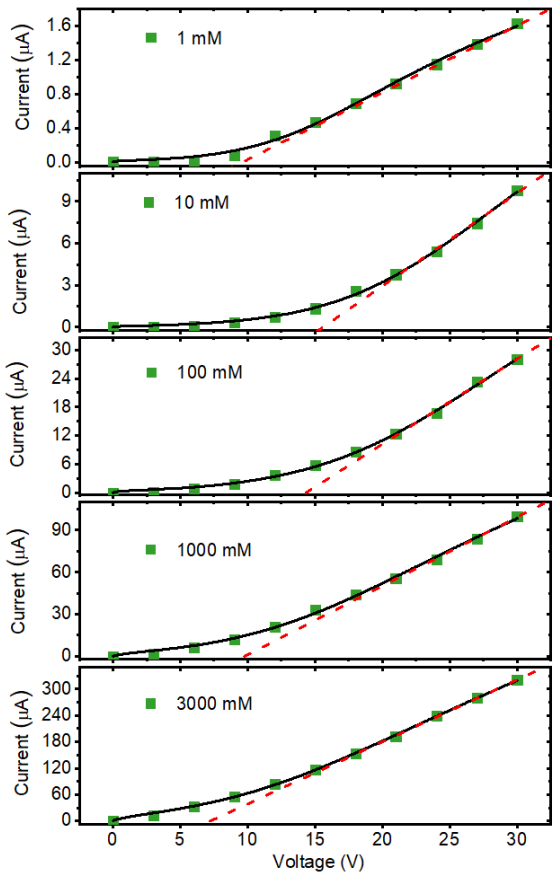

FIG. S5. Here we showed evaluation the critical voltage of conductance transition. We have a linear fitting (red dashed line) of the I-V curves at voltage over 15V, where shows a good agreement of linear increase. The fitted line crossing with the X-axis which we considered as the transition voltage V_C.

IV. CHARACTERIZATION OF THE CHANNEL DIAMETER BY ISOTHERM ADSORPTIONS

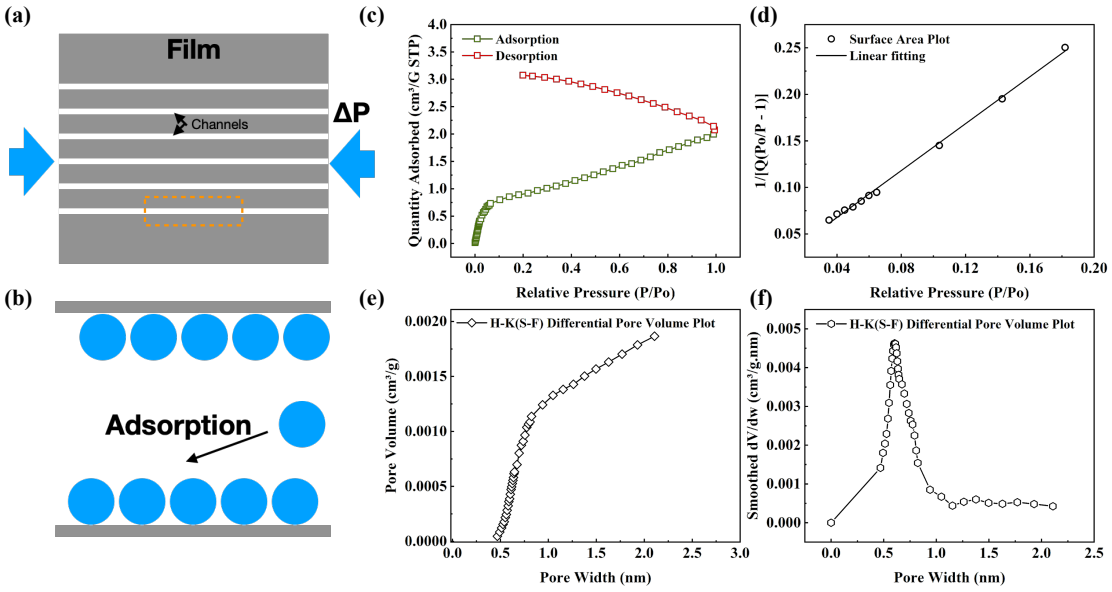

FIG. S6. The characterization of channel size by isotherm adsorption of CO2 gas molecules.

The FigS6.a schematically illustrated the angstrom scale channels with applied pressure of CO_2. The gas molecules forms Langmuir adsorption (b) to the surface, thus enables to measures the quantity of adsorbent to under a relative pressure ($P/P0$), where P_0 is the atmosphere pressure. We first vacuum the chamber of specimens, and gradually filled with CO_2 with applied pressure P.

For each step, we remained for over 15 seconds to reach an equilibrium state of adsorption. Fig S6(c). shows the absorbent volume for each steps having a kinetic of the isotherm adsorption by CO_2. To maximize the enough surface area, we fabricated over 24 films with thickness of $12\mu m$ for each film, with an overall surface area of over $15cm^2$. We noted that the desorption process has a clear deviation from the adsorption curves, which we attributed to the penetration of CO_2 to the polymer at surface. Pretty clear wrinkles were found on the polymer foil after the experiments, possible caused by the stress due to desorption of gas molecules. According to the Langmuir adsorption equation, we could derive the by equation shown below.[[S1]]

$$\frac{p}{v} = \frac{p}{v_m} + \frac{1}{v_m b} \tag{S1}$$

where $b = \frac{KA}{a_m f} e^{\epsilon_d / RT}$ and $K = N/(2\pi MRT)^{1/2}$. The p, M, R, T, v_m, v are the applied pressure, Relative molecular mass, Molar gas constant, temperature, monolayer capacity and adsorption quantity. We derived the surface to bulk ratio of our specimens are $2.986 \pm 0.049 m^2/g$.

According to the H-K equation in a cylinder channel, we could derive the radius of the channel. [[S2]]

$$RTln(p/p_0) = \frac{3\pi K}{4} \times \sum \frac{1}{2k+1} (1 - \frac{2d_0}{r}^{2k} - [\frac{2la_k}{32}(\frac{2d_0}{r})^{10} - (\beta_k \frac{2d_0}{r})^4]) \tag{S2}$$

where r is the radius of the channel. The α and β are the calculated values from E-P models. Finally, we found the radius of channel distributed from 0.5nm to 1nm, with a most probable diameter of 0.60nm. The radius smaller than 0.48nm are difficult to be measured. Thus, we take the most probable value of the pore radius as 0.6nm, approving that are in the angstrom scale channel.

V. IONIC TRANSPORT BY MOLECULAR DYNAMICS SIMULATION

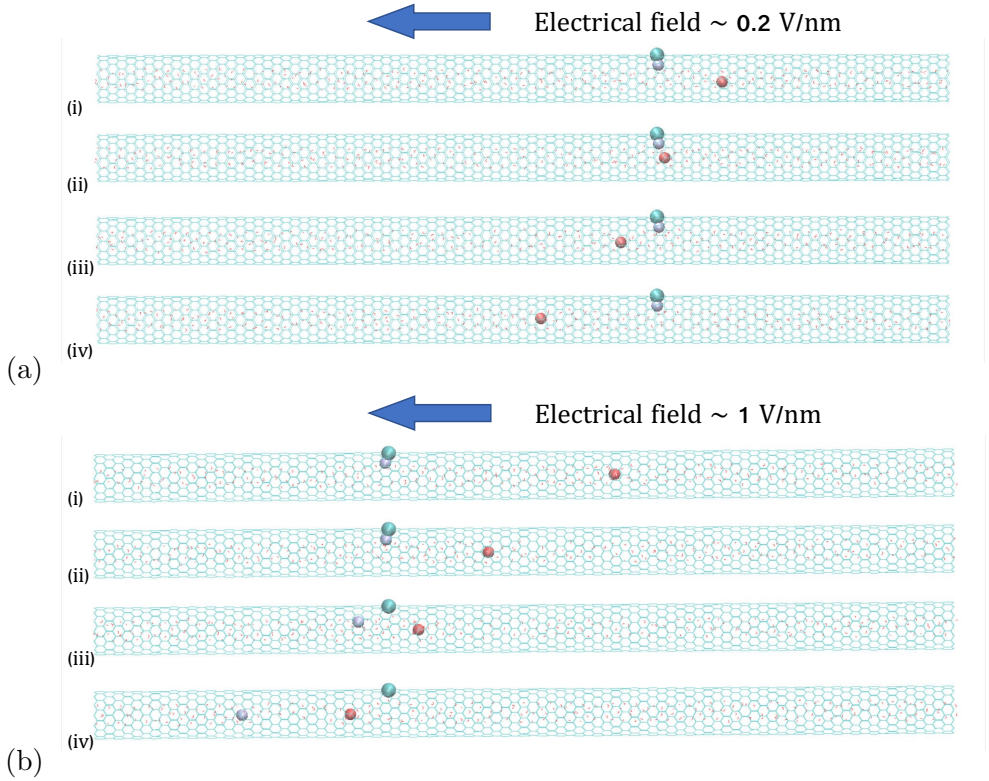

FIG. S7. (a) the free ion entered the CNT channel, however blockade by the bound ion in single file channel. When the bound ion leaving space for the transport of free ions, the latter one passing though the bound ion forming electrical current. Thus, this indicates the conduction of channels are independent of the surface charge density, which the conductance possible is far smaller than the predicted values due to the ionic Coulomb blockade. (b) As rising of the electrical field, the probability of releasing the bound ion increases, resulting opening of channels for ion transport.

We build a single (14,0) zigzag carbon nanotube (CNT) with effective diameter of $0.55nm$ in LAMMPS package to study the ion transport. We set a periodic boundary of CNT in all directions with a unit length of 2nm. The temperature was set as 298 K and 1 atm in our simulation. To simply illustrate the Coulomb Blockade in the CNT, we randomly placed a carbon atom on CNT surface been charged with an elementary charge e. We found the counterion is strongly bound to the surface charge, blocking the path for the ionic conduction. It needs a strong external electrical field to release the bound ion. At small electrical field, the cations oscillated near the bound ion and crossing the bound ion forming current. In

such low electrical field, the conduction relies on the density of free ions (C_b) in the CNT, independent of the surface charge density. However, the bound ion may block the channel for ion transport, in particular the size of our latent ion track channels has a distribution. From the conduction of the high resistance state (HR), we could calculate the conductive channel is $\sim 0.1\%$ of the total number of channels estimated from the irradiation density and area of the membrane contact to solution. However, as the electrical field increases, when another cation passing by the bound ion, there is a probability that the bound ions can be released forming additional current. In such cases, the channels have a probability of been opened for conductive. The fitted conductance g suggested the 60% opened for conduction, calculated by diameter of 0.6nm and bulk conductivity κ_b. The reduction of fitted conductivity may be possible caused by the reduction of ion mobility in the angstrom-scale channel. According to our fittings, the conductance g predicts the conduction that all of channel been conductive. We will have the radius of channel is ~ 0.55nm, close to the values measured by the isotherm adsorption shown in Fig. 1b. The transition electrical field in CNT seems to be much higher than in the PET membrane, due to the vacuum area in CNT resulting a stronger Coulomb interactions between bound ion and surface charge. However, the PET membrane is able to adsorbed water thus having much weaker Coulomb interactions and lower potential well to release the bound ion.

VI. IONIC TRANSPORT MECHANISMS BY KRAMER'S ESCAPING APPROXIMATION

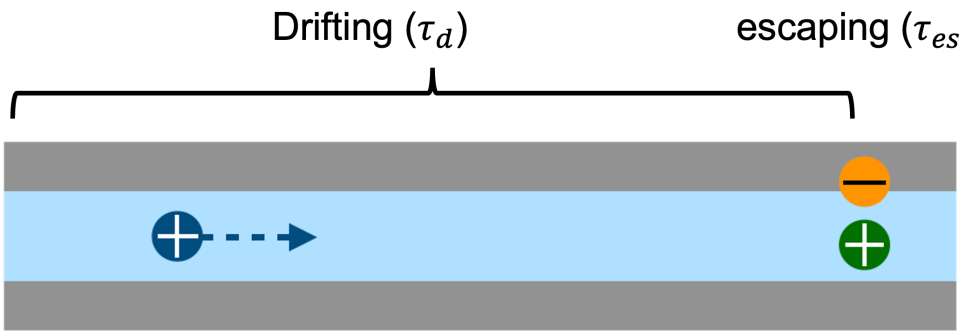

FIG. S8. Schematic picture of the ion transport through a channel.

Figure S8 showed the scheme image of the ion transport through an angstrom-scale channel. As reported, once the radius of channel getting close to the hydrated ion, the ion may cost extra energy to excited passing through the channel.[S3] This energy barrier maybe caused by dehydration of the ions, self-energy increase in angstrom-scale channel, Wien-effects of the ion-pairs. We first considered an equivalent potential barrier that caused by the either one or multiple effects above, with height of the potential ΔU_0. Consider a free monovalent ion in the channel, we could calculate the ion fluxes by following equation

$$I = N\frac{CA_{ch}Le}{\tau_d + \tau_{es}} \tag{S3}$$

where the τ_d and τ_{es} are the time of drifting through the channel and the escaping time from the energy barrier, with number of channels N distributed in the membrane. The drift time of ion in the channel can estimated by

$$\tau_d = L/\mu E \tag{S4}$$

where the L, e, μ, E are the length of channel, elementary charge, mobility of ions and electrical field. Here we ignored the entrance effects of the ionic conduction, as we have an "infinite" long channels where radius ($\sim 1nm$) much smaller than the length of channel ($\sim 10\mu m$).

$$\frac{\partial W}{\partial t} = D\left[\frac{\partial}{\partial z}(\frac{1}{k_BT}\frac{\partial U}{\partial z}W) + \frac{\partial^2 W}{\partial z^2}\right] \tag{S5}$$

The time of escaping according to Kramer's approximation can be expressed by [[S4]]

$$\tau_{es} = 2\pi(|U''_{x_{max}}|U''_{x_{min}})^{-1/2}e^{\Delta U/k_BT} \tag{S6}$$

where the k_B, T are Boltzmann constant and temperature. The potential includes the energy barrier and external potential distribution along the channel, $\Delta U = \Delta U_0 - eEd_{es}$, where the ΔU_0 is the energy barrier of the angstrom-scale channel and d_{es} is the distance that ions moving from minimum to the maximum of the energy barrier.

Thus, we can rewrite the equation S3 considering the total number of ions as follows. Here we need to count the bound ions, since it has probability of been released by the electrical field and contribute to the conduction current.

$$I = \frac{N(\frac{CA_{ch}e\mu}{L})V}{1 + \frac{2\pi\mu V}{L^2}(|U''_{x_{max}}|U''_{x_{min}})^{(-1/2)}e^{\Delta U/k_BT}} \tag{S7}$$

Thus, we have a simple formula to fit the experimental data.

$$I = \frac{gV}{1 + kVe^{-bV}} \tag{S8}$$

With all fitted parameters of conduction g

$$g = N\frac{CA_{ch}e\mu}{L} \tag{S9}$$

where N is the number of channels, and the A_{ch} is the cross-sectional area of a single channel, C includes the concentration of ions from bulk solution C_b and bound ions due to attraction of the surface charge $C_\Sigma = \frac{2\Sigma}{re}$.

$$k = \frac{2\pi\mu V}{L^2}(|U''_{x_{max}}|U''_{x_{min}})^{(-1/2)}e^{\Delta U/k_BT} \tag{S10}$$

Considering the constant in equation S10, we could rewrite the equation as follows.

$$k \sim \mu e^{\Delta U/k_BT} \tag{S11}$$

To directly compare with the different monovalent ions, we normalized the mobility of Li^+, Cs^+ ions by K^+ according to above equation, shown in the figure 4a. The fitted factor b is proportional to the charge of ion e, and equivalent escaping distance d_{es} that is determined

by the interaction of ion-pair. It remains as a constant as density of the salt concentrations that we found in the experiments.

$$b \sim \frac{ed_{es}}{k_B T} \tag{S12}$$

VII. THE CONDUCTION AT SMALL ELECTRICAL FIELD

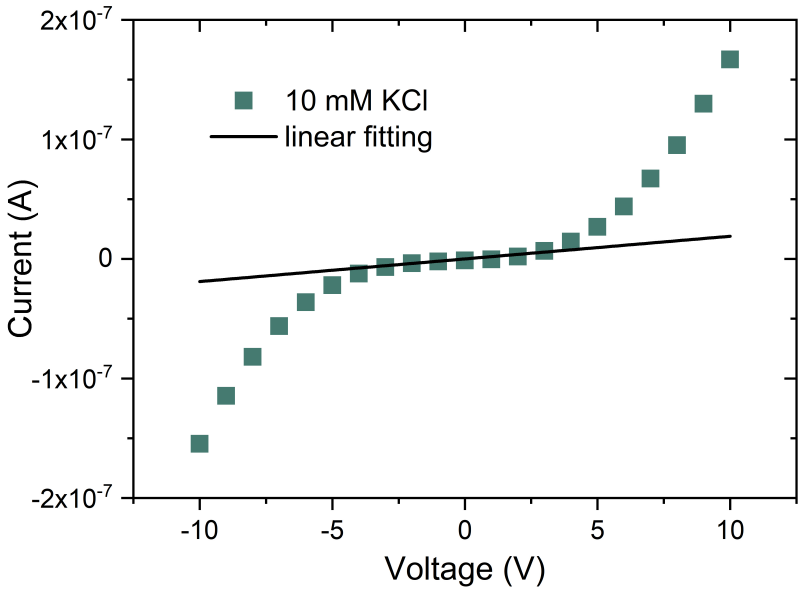

FIG. S9. An example of linear fits of I-V curves at applied voltage smaller than $\pm 3V$.

VIII. THE I-V CURVES WITH DIFFERENT FILM THICKNESS

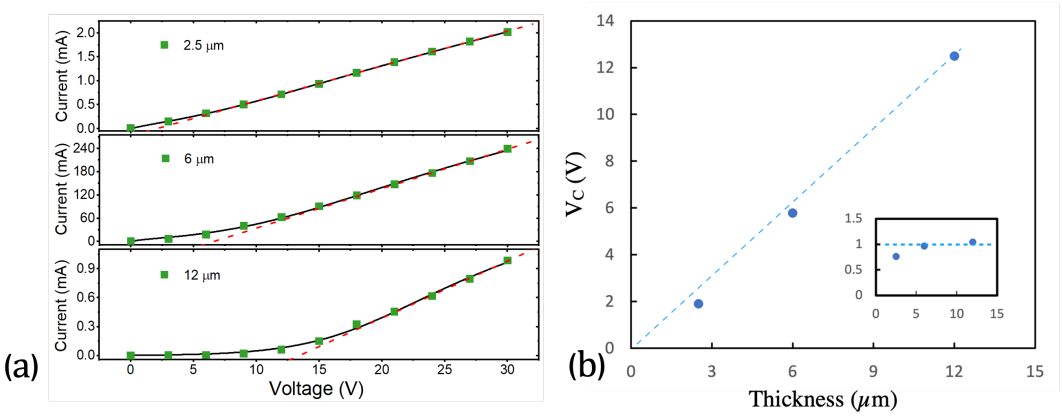

FIG. S10. the typical I-V curves in various thick of film. (b) shows the transition voltage of conductance as a function of the thickness.

We investigated the conduction with the latent ion track film with thickness from $2.5\mu m$, $6\mu m$ and $12\mu m$, including the transition voltage V_C. The typical I-V curves with 10mM KCl solution at pH 5.0 were shown in the Figure S10. It needs to be noted that the current amplitude is over an order higher than of the 12µm-thick membrane, which is due to the density of latent ion track channel of former two specimens are $5 \times 10^9 cm^{-2}$ over an order higher than the specimens of $12\mu m$ thickness. It nearly turns to be Ohmic resistor at $2.5\mu m$ thick liquid film. We noted that the V_C gradually decreases as the thickness shown in Fig S10b, agreed well with the linear increases as the thickness. We derived the critical electrical field $E_C = V_C/L$ as a constant ($\sim 1V/\mu m$) shown in the inset figure of Fig S10b. Our results indicated that the similar phenomena in our experiments were possibly difficult been observed in the nanopore on single layer 2D materials, as it is nearly impossible to measure the current by operating 0.1mV crossing an atomic thick membrane ($\sim 0.1nm$), remaining the EC of $\sim 1V/\mu m$.

IX. ION MOBILITY IN CHANNELS

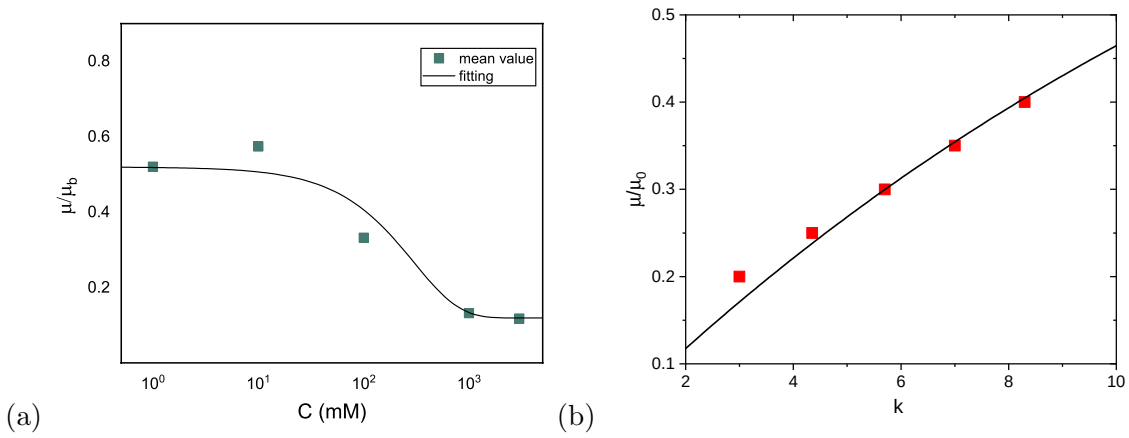

(a) (b)

FIG. S11. (a) the ion mobility μ derived from the fitted conduction g, normalized by the mobility in bulk solution μ_b as a function of concentration. We took a mean value from three different types of ions to obtain the reduction factors. The solid line is a fitting factor $\mu/\mu_b = 0.12 + 0.4e^{-C/210}$, where C is in unit of mM. The calculated ion mobility is generally smaller than the bulk value, possibly due to the reduction of ion mobility in confinements [S5]. (b) the variation factor of ion mobility μ/μ_0 as a function of k, $\mu/\mu_0 = 1 - e^{-k/16}$ which gradually decreases at small k, matching well with the tendency of reduction as we found in high concentrations (low k). The μ_0 indicates the ion mobility in diluted salt concentrations as shown in figure S11a.

X. REFERENCES

[S1] I. Langmuir, THE ADSORPTION OF GASES ON PLANE SURFACES OF GLASS, MICA AND PLATINUM., Journal of the American Chemical Society **40**, 1361 (1918).

[S2] G. H. KAWAZOE, Method for the calculation of effective pore size distribution in molecular sieve carbon, Journal of Chemical Engineering of Japan **16**, 470 (1983).

[S3] N. Kavokine, S. Marbach, A. Siria, and L. Bocquet, Ionic coulomb blockade as a fractional wien effect, Nature Nanotechnology **14**, 573 (2019).

[S4] H. Risken, *The Fokker-Planck Equation*, edited by H. Haken, Springer Series in Synergetics, Vol. 18 (Springer Berlin Heidelberg, Berlin, Heidelberg, 1984).

[S5] P. M. Bungay and H. Brenner, The motion of a closely-fitting sphere in a fluid-filled tube, International Journal of Multiphase Flow **1**, 25 (1973).